DOI: 10.1002/asia.200600371

Spin-Crossover Physical Gels: A Quick Thermoreversible Response Assisted by Dynamic Self-Organization

Tsuyohiko Fujigaya,[a] Dong-Lin Jiang,*[b] and Takuzo Aida*[a]

Abstract: Iron(II) triazolate coordination polymers with lipophilic sulfonate counterions with alkyl chains of different lengths have been synthesized. In hydrocarbon solvents, these polymers formed a physical gel and showed a thermoreversible spin transition upon the sol–gel phase transition. The formation of a hydrogen-bonding network between the triazolate moieties and sulfonate ions, bridged by water molecules, was found to play an important role in the spin-crossover event. The spin-transition temperature was tuned over a wide range by adding a small amount of 1-octanol, a scavenger for hydrogen-bonding interactions. This additive was essential for the iron(II) species to adopt a low-spin state. Compared with nongelling references in aromatic solvents, the spin-crossover physical gels are characterized by their quick thermal response, which is due to a rapid restoration of the hydrogen-bonding network, possibly because of a dynamic structural ordering through an enhanced lipophilic interaction of the self-assembling components in hydrocarbon solvents.

Keywords: gels · phase transitions · self-assembly · spin crossover · triazoles

Introduction

The spin states of several complexes of first-row transition metals are known to switch between low-spin and high-spin states in response to external perturbations caused by changes in temperature and pressure or photoexcitation.[1] This phenomenon, referred to as spin transition or spin crossover, leads to changes in the magnetic and optical properties of the materials and has great potential for memory, display, and sensor applications.[2] One of the primary requisites for spin-crossover materials is an abrupt spin transition, for which spin-active sites should be connected strongly with one another to create a high cooperativity.[3] Solid or crystalline inorganic materials have been studied most extensively so far as potential spin-crossover materials,[1] and some show an abrupt spin transition in a narrow temperature range. On the other hand, recent attention has been focused on soft materials with spin-crossover properties, as these materials can be processed easily by casting and tuned by molecular design.[4] However, because of a larger freedom of molecular ordering, one may anticipate a possible loss of long-range cooperativity among the spin-transition sites, with the result of non-abrupt spin crossover, as often observed in solution.[2a] Recently, we reported the first example of self-organized dendritic spin-crossover materials, whose spin-transition properties are controlled by the dimensions of the dendritic ligand.[5] Notably, an abrupt spin transition occurred in a narrow temperature range upon the proper choice of a dendritic ligand that can densely fill the unit cell to form the spin-active site. In the course of this study, we happened to notice that nondendritic references **3b–d** (Scheme 1), which have a sulfonate counterion with a lipophilic long alkyl chain, form a physical gel in paraffinic solvents such as hexane, octane, dodecane, and hexadecane.[4c] Herein we report that these physical gels are capable of magneto–optical switching upon sol–gel phase transition. Unlike reported examples with inorganic crystalline materials, the spin crossover can be repeated many times without deterioration. Furthermore, it occurs in quick response to a temperature change. We highlight that these interesting features take great advantage of a dynamic self-as-

[a] T. Fujigaya, Prof. Dr. T. Aida
Department of Chemistry and Biotechnology
School of Engineering, The University of Tokyo
7-3-1 Hongo, Bunkyo-ku, Tokyo 113-8656 (Japan)
Fax: (+81) 3-5841-7310
E-mail: aida@macro.t.u-tokyo.ac.jp

[b] Dr. D.-L. Jiang
Aida Nanospace Project
Exploratory Research for Advanced Technology (ERATO)
Japan Science and Technology Agency (JST)
2-41 Aomi, Koto-ku, Tokyo 135-0064 (Japan)
Fax: (+81) 3-3570-9183
E-mail: jiang@nanospace.miraikan.jst.go.jp

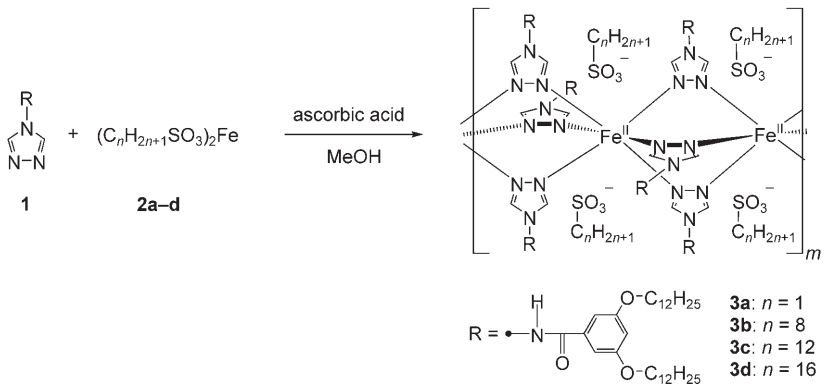

Scheme 1. Synthesis of the iron(II) triazolate coordination polymers with sulfonate counterions **3a–d**.

sembly event through hydrogen-bonding and lipophilic interactions.

Results and Discussion

The iron(II) complexes **3a–d** (Scheme 1) were synthesized by mixing the triazole ligand **1** with the iron(II) salts **2a–d** in MeOH containing a small amount of ascorbic acid and were obtained as purple precipitates. Infrared spectroscopy of **3a–d** showed a red shift of the C=N stretching vibrational band from 1552 to 1561 cm^{-1}, which is characteristic of iron(II) triazolate complexes.[6] Peaks in the X-ray absorption fine structure (EXAFS) spectra of the solid samples of **3a–d** at 1.8, 3.5, and 7 Å were assigned to Fe–N, Fe–Fe, and linear Fe–Fe–Fe scatterings, respectively (Figure 1). Therefore, it was concluded that **3a–d** are coordination polymers with multiple iron(II) sites.

The solid samples of **3a–d** were purple at 23 °C, as is typical of low-spin iron(II) species. Compounds **3b–d** were highly soluble in aromatic solvents such as benzene, toluene, and *m*-xylene, and the resulting purple solutions at 23 °C all displayed an absorption band at around 540 nm due to a $^1A_{1g}$–$^1T_{1g}$ d–d transition characteristic of low-spin iron(II) species. In contrast, although compound **3a** was soluble in the above aromatic solvents, the solutions were pale-yellow at 23 °C. On the other hand, **3b–d**, which have a lipophilic sulfonate counterion, formed a purple transparent gel in paraffinic solvents at 23 °C even at such a low concentration as 0.6 wt %, whereas no gelation occurred with **3a** with the nonlipophilic counterion $CH_3SO_3^-$. For example, electronic absorption spectroscopy of a dodecane gel of **3c** (0.6 wt %) showed a characteristic band at 537 nm due to the d–d transition of the low-spin state (Figure 2). Upon heating to

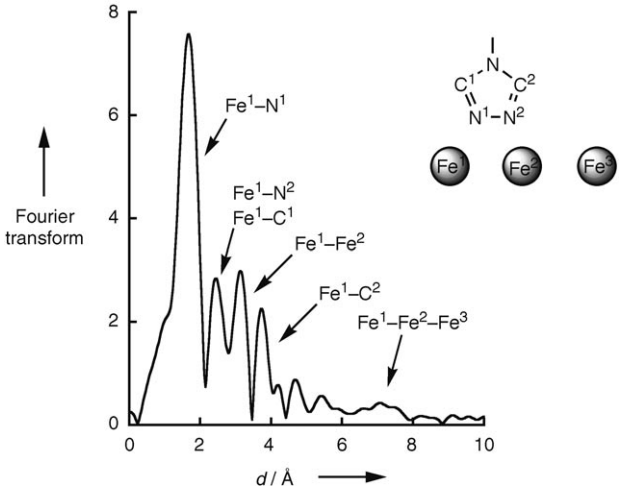

Figure 1. EXAFS profile of a solid sample of **3c**.

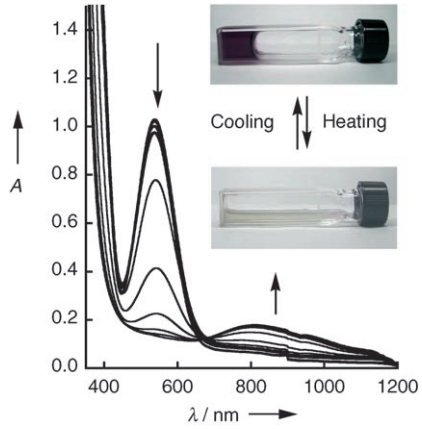

Figure 2. Change in the electronic absorption spectrum of a gel of **3c** in dodecane (0.6 wt %) upon heating from 15 to 80 °C.

International Advisory Board Member

Takuzo Aida *received his PhD from the Univ. of Tokyo in 1984 and became Prof. of Macromolecular Chemistry there in 1996 and the director of the JST ERATO NANOSPACE project in 2000. His research interests include supramolecular chemistry, nanomaterials, and molecular/biomolecular machines. He has received several awards, including the Wiley Polymer Chemistry Award (1999), the IBM Science Award (1999), the Tokyo Techno Forum Award Gold Medal (2001), the Inoue Prize for Science (2005), and the Arthur K. Doolittle Award (2005).*

"Here comes a top-quality international journal for chemistry that is of Asia as well as the world. A treasure island of creativity and innovation is right here."

80 °C, the purple gel collapsed to give a pale-yellow clear solution. Variable-temperature absorption spectroscopy on heating from 15 to 80 °C showed the appearance of a broad band centered at 850 nm as a result of a $^5T_{2g}$–^5E_g d–d transition of the high-spin state, at the expense of the low-spin absorption band at 537 nm (Figure 2). On cooling to 15 °C, the hot solution immediately turned into a purple transparent gel, recovered the low-spin absorption band at 537 nm, and lost the broad high-spin absorption band at 850 nm. Such a thermally induced discoloration–coloration cycle could be repeated many times without any sign of deterioration. Plots of the absorbance at 537 nm versus temperature for heating and cooling events (●, Figure 3a) indicate that the spectral change is centered at 55 °C (T_c) in a narrow temperature range (ΔT) of 45–65 °C. A virtually identical temperature-dependent color change was observed over a wide range of concentrations of **3c**, from 0.6 to 40 wt %. The observed thermochromic behavior is clearly due to the spin transition. In fact, when a dodecane gel of **3c** (40 wt %) was heated from 250 K, its magnetic moment (M) increased abruptly at 330 K (57 °C) from -3.4×10^{-3} to 3.8×10^{-3} emu g^{-1}, in the narrow temperature range of 320–340 K (Figure 3b).[7] Upon cooling from 360 K, an abrupt drop in the magnetic moment occurred at 330 K (57 °C) from 3.8×10^{-3} to -2.5×10^{-3} emu g^{-1}. We found that compounds **3b** (▲, Figure 3a) and **3d** (■, Figure 3a) display very similar thermal spin-transition behavior upon gelation in paraffinic solvents to that of **3c** (●, Figure 3a). In sharp contrast, nongelling **3a** in dodecane remained in a high-spin state and a pale-yellow color over a wide temperature range (○, Figure 3a).

Polarized optical microscopy of the dodecane gel of **3c** (40 wt %) showed the characteristic texture of a liquid-crystalline mesophase (Figure 4). Upon heating to induce the gel-to-sol phase transition, the liquid-crystalline texture disappeared completely at 62 °C. A rheological study at 25 °C showed that the dynamic storage (G') and loss (G'') curves both contain a plateau region with no sign of relaxation over a wide range of angular frequencies from 0.1 to 100 rad s^{-1} (Figure 5). These observations suggest that the system consists of a long-range alignment of cylindrical **3c**. Figure 6 shows temperature-dependent rheological properties of the gel at a fixed angular frequency (ω) of 10 rad s^{-1}.

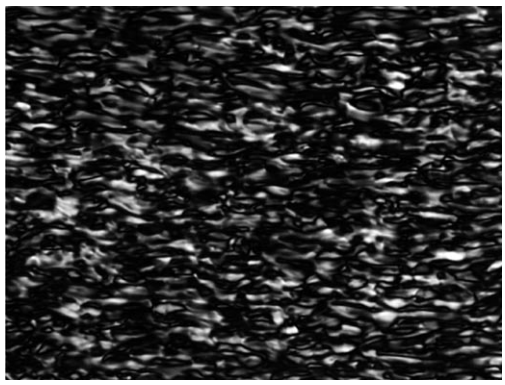

Figure 4. Polarized optical micrograph of a gel of **3c** in dodecane (40 wt %) at 25 °C.

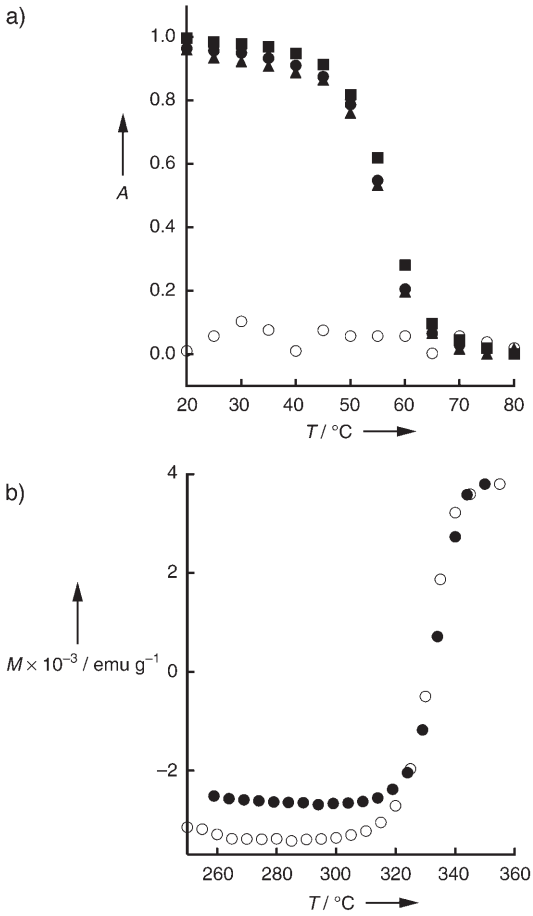

Figure 3. Changes in a) the absorbance at 537 nm of **3a** (○), **3b** (▲), **3c** (●), and **3d** (■) in dodecane (0.6 wt %) and b) the magnetic susceptibility of **3c** (40 wt %) upon heating (○) and cooling (●).

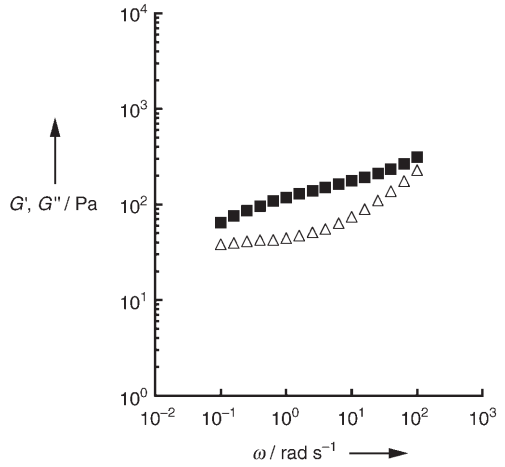

Figure 5. Rheological properties of a gel of **3c** in dodecane (20 wt %): angular frequency (ω) dependencies of storage (G'; ■) and loss moduli (G''; △) at 25 °C.

CHEMISTRY
AN ASIAN JOURNAL

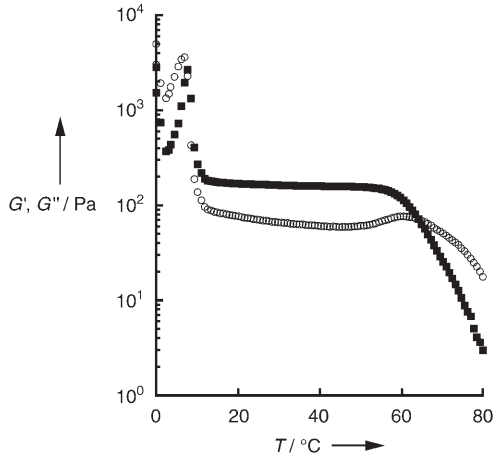

Figure 6. Rheological properties of a gel of **3c** (20 wt%) in dodecane: temperature dependencies of storage (G'; ■) and loss moduli (G''; ○).

When the temperature was lower than 60 °C, the G' and G'' curves both had a plateau region in which the G' value remained larger than the G'' value as an indication that the physical gel is elastic. When the temperature exceeded 60 °C, the G' and G'' values both tended to drop. Plots of the G' value allowed the determination of the cross-point ($G' = G''$) temperature of 62 °C. After this cross point, the G' value became smaller than the G'' value, which indicates the occurrence of a gel-to-sol phase transition. As the cross-point temperature of 62 °C agrees well with the spin-crossover temperature ($T_c = 57$ °C), we can conclude that the iron(II) species in the gel and sol states prefer to adopt low-spin and high-spin states, respectively.

A hydrogen-bonding network plays an important role in the spin-crossover event.[8] Infrared spectra of the dodecane gel of **3c** (40 wt%) at 25 °C showed vibrational bands at 1213 and 1104 cm^{-1} due to RSO_3^- and the C–H bond of the triazolate,[9] respectively (Figure 7). A broad band at 3500 cm^{-1} can be assigned to water molecules involved in the hydrogen-bonding network with RSO_3^- and the triazolate species (Scheme 2).[10] Upon heating, the vibrational bands due to RSO_3^- and the C–H bond of the triazolate were red-shifted at 45–50 °C toward 1207 and 1080 cm^{-1}, respectively, whereas that assigned to the hydrogen-bonded water molecules disappeared completely (Figure 7). In contrast, a nongelling dodecane solution of compound **3a** did not display such an infrared spectral profile characteristic of hydrogen-bonded species (Figure 8).

Alcohols are known to scavenge hydrogen bonds. When a small amount of 1-octanol was added to the system, the gel collapsed immediately to form a solution (Figure 9, inset). Infrared spectroscopy of the resulting solution showed red shifts of the vibrational bands assigned to the hydrogen-

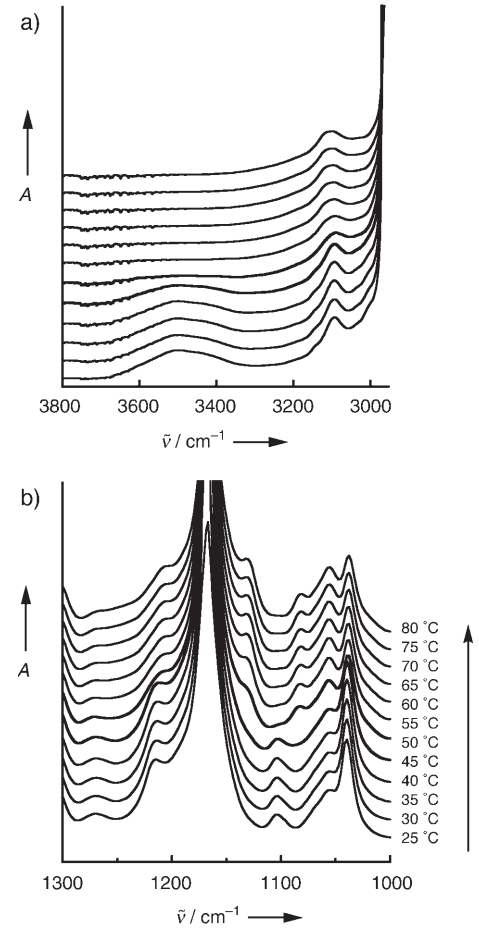

Figure 7. Changes in the infrared spectrum in the regions a) 3800–2950 cm^{-1} and b) 1300–1000 cm^{-1} of a gel of **3c** in dodecane (40 wt%) upon heating.

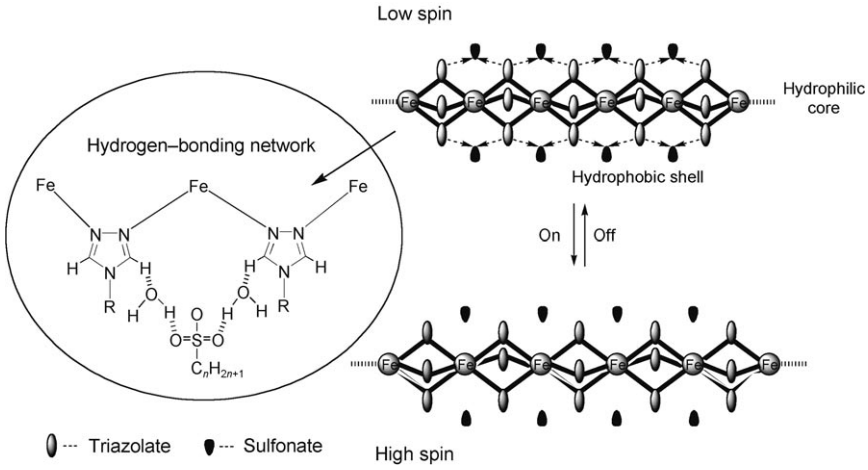

Scheme 2. Proposed schematic structures of spin-crossover species **3b–d**.

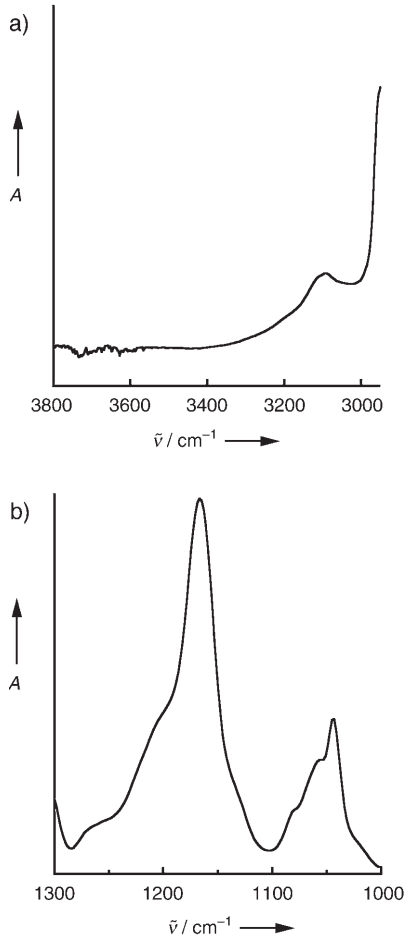

Figure 8. Infrared spectrum in the regions a) 3800–2950 and b) 1300–1000 cm^{-1} of a solution of **3a** in dodecane (40 wt%) at 25°C.

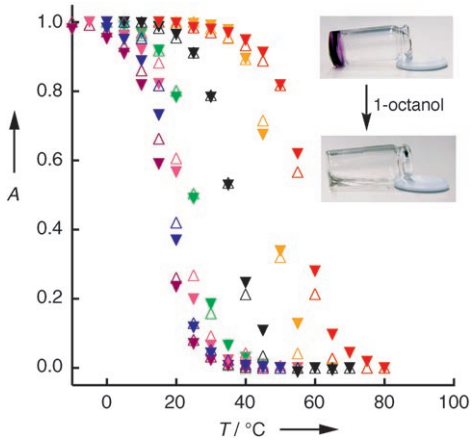

Figure 9. Changes in the absorbance at 537 nm of a gel of **3c** in dodecane (0.6 wt%) in the presence of 1-octanol at [1-octanol]/[Fe]=0 (red), 2 (orange), 6 (pink), 18 (green), 30 (black), 42 (blue), and 60 (purple) on cooling (open triangles) and heating (filled triangles). The inset shows pictures of the sample before and after the addition of 1-octanol ([1-octanol]/[Fe]=30).

bonded species (Figure 10). These red shifts suggest a breakdown of the hydrogen-bonding network by 1-octanol. The pale-yellow color of the solution indicates that the iron(II)

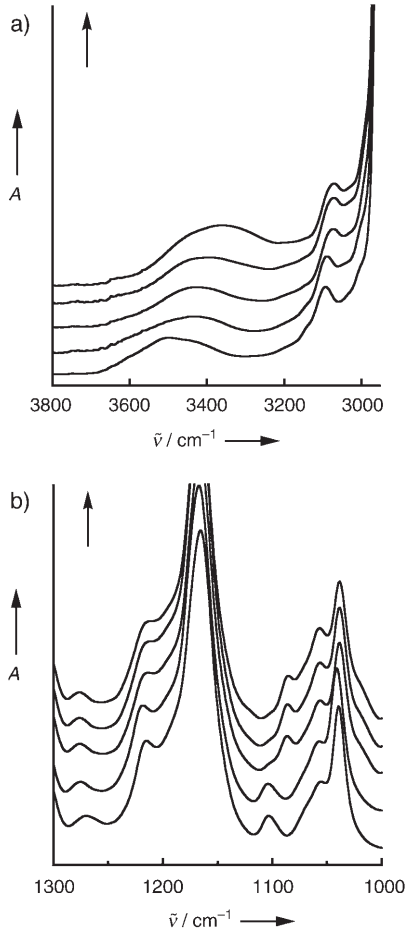

Figure 10. Changes in the infrared spectrum in the regions a) 3800–2950 and b) 1300–1000 cm^{-1} of a gel of **3c** in dodecane (40 wt%) at 25°C upon the addition of 1-octanol at [1-octanol]/[Fe]=0, 6, 18, 24, and 30.

species was in a high-spin state. Upon titration of a dodecane gel of **3c** (0.6 wt%) with 1-octanol at 25°C, a broad absorption band centered at 850 nm due to the high-spin iron(II) species appeared again at the expense of the low-spin absorption band at 540 nm (Figure 11). As shown by variable-temperature absorption spectra of the titrated samples (Figure 9), an increase in the concentration of 1-octanol resulted in the lowering of the spin-transition temperature from 55 to 15°C. It is most likely that the hydrogen-bonding network around the spin-active sites locks the Fe–N bond length at a distance that favors the low-spin iron(II) state. Upon heating to induce the gel-to-sol phase transition, a thermal breakdown of this hydrogen-bonding network takes place, thereby permitting the elongation of the Fe–N bond as required for the transition to the high-spin state.

The spin-crossover physical gels are characterized by their quick thermal response. For example, when a dodecane gel of low-spin **3c** (0.6 wt%) was heated from 40 to 80°C, and the resulting solution of high-spin **3c** was cooled to 40°C, the spectral change at 540 nm due to the recovery of the low-spin state was completed within only 2 min (○, Figure 12). As good references, we found that nongelling

CHEMISTRY
AN ASIAN JOURNAL

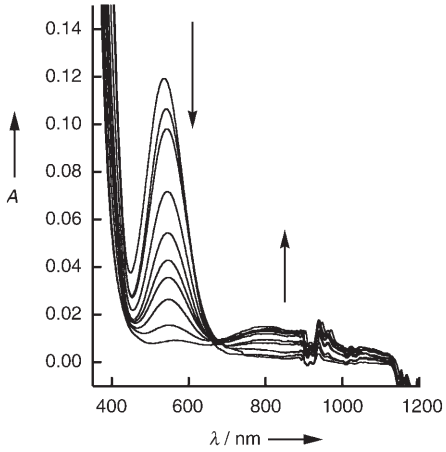

Figure 11. Change in the electronic absorption spectrum of a gel of **3c** in dodecane (0.6 wt%) at 25°C upon the addition of 1-octanol at [1-octanol]/[Fe] = 0–60.

solutions of **3b–d** in aromatic solvents display a thermoreversible spin transition at 30°C (Figure 13). The changes in their absorption spectra for the high-to-low-spin transition

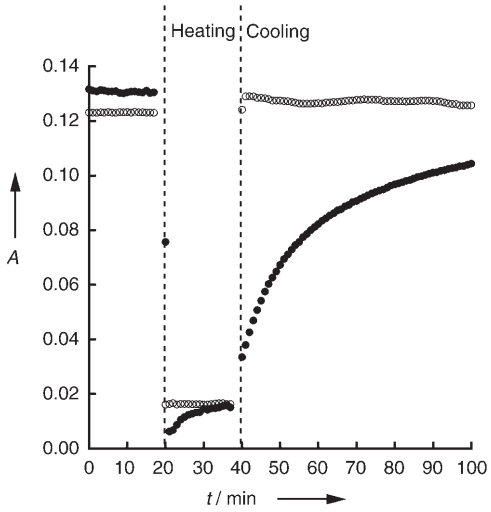

Figure 12. Time-dependent changes in the absorbance of **3c** in *m*-xylene (●) and dodecane (○) upon rapid heating and cooling, monitored at 540 and 537 nm, respectively.

were extremely sluggish. For example, when a solution of low-spin **3c** (0.6 wt%) in *m*-xylene at 20°C was heated to 50°C and then cooled rapidly to 20°C, the spectral change at 540 nm did not subside even in 300 min (●, Figure 12). Infrared spectroscopy allowed us to confirm the presence of a hydrogen-bonding network in the solution of low-spin **3c** in *m*-xylene (Figure 14). For the quick thermal response of the spin-crossover gels, we assume that the restoration of the hydrogen-bonded network after its thermal breakdown may be facilitated by a lipophilic interaction of the spin-active

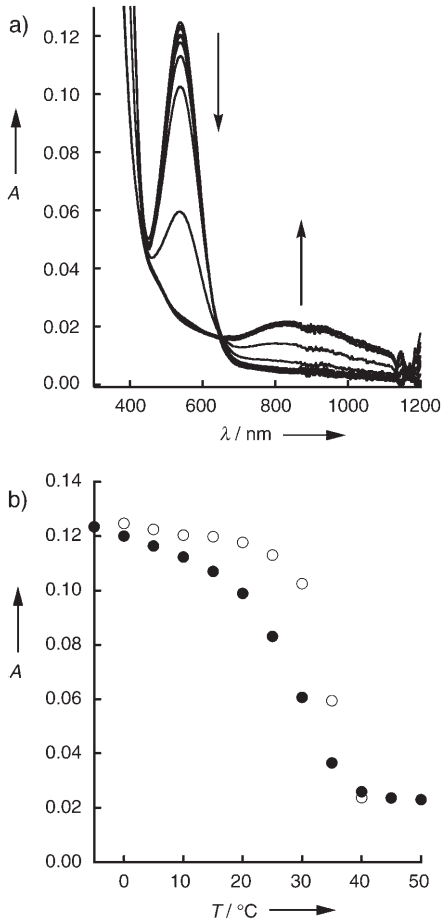

Figure 13. a) Change in the electronic absorption spectrum of **3c** as a solution in *m*-xylene (0.6 wt%) on heating from −5 to 50°C. b) Changes in the absorbance at 540 nm of **3c** as a solution in *m*-xylene (0.6 wt%) on heating (○) and cooling (●).

coordination polymers. This lipophilic interaction is possibly enhanced in hydrocarbons.

As already described, **3a** with a $CH_3SO_3^-$ counterion does not form a gel. The lipophilic long alkyl chains in the sulfonate counterions of **3b–d** therefore seem to have an important role in the gelation. In hydrocarbon solvents, the iron(II) triazolate coordination polymer within a paraffinic coat probably co-assembles through a lipophilic interaction with sulfonate counterions with a C_8, C_{12}, or C_{16} alkyl chain to form a cylindrical core–shell architecture, in which water molecules are incorporated into the core and form the hydrogen-bonding network between the RSO_3^- triazolate units. The latter units take part in hydrogen bonding through their acidic C–H bonds (Scheme 2). For the gelation, such paraffinic cylinders co-assemble, again through lipophilic interactions, to grow into a macroscopic network structure. Therefore, although the hydrogen-bonding network is broken thermally to allow a low-to-high-spin transition, a molecular ordering triggered by such a lipophilic force could facilitate restoration of the hydrogen-bonding network, which would lead to the quick recovery of the low-spin state. Overall, the spin crossover appears to be coupled

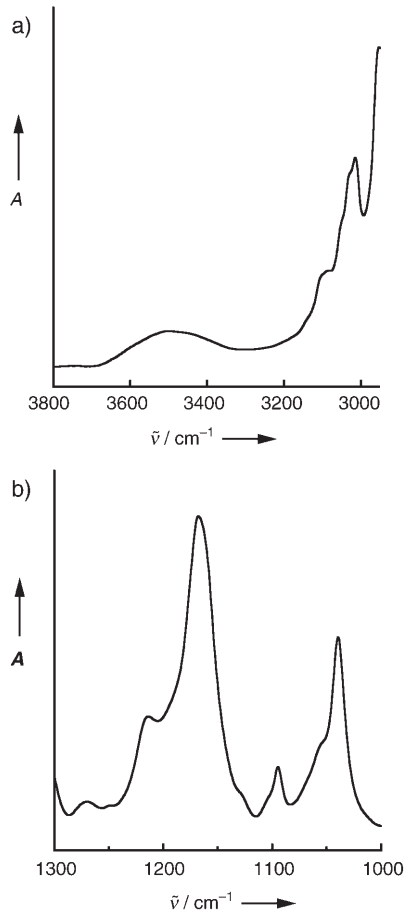

Figure 14. Infrared spectrum in the regions a) 3800–2950 and b) 1300–1000 cm^{-1} of **3c** as a solution in *m*-xylene (40 wt %) at 25 °C.

with the sol–gel phase transition. Roubeau et al. reported a spin-crossover physical gel with an iron(II) triazolate coordination polymer that contained tolylsulfonate ions.[4c] In this case, the spin transition and phase transition do not appear to be coupled with one another, as their transition temperatures are as far apart as 20–100 °C depending on the concentration. It is interesting to note that the very different thermal behavior of their spin-crossover system is caused by a rather small structural difference in the self-assembling components.

Conclusions

In summary, we have reported novel spin-crossover physical gels that undergo a thermoreversible spin transition upon sol–gel phase transition in hydrocarbon solvents. A paraffinic iron(II) triazolate coordination polymer hydrogen-bonded with lipophilic sulfonate counterions was used for these studies. The spin crossover can be repeated many times without deterioration, as a volume change of the spin-active sites upon spin transition would not lead to an irreversible structural deformation as typically observed for crystalline solid materials. Furthermore, because of an enhanced lipophilic interaction in hydrocarbons, the spin crossover occurs in quick response to a temperature change. The introduction of stimuli-responsive functionalities may allow the fabrication of novel spin-crossover soft materials, for example, for sensory applications.

Experimental Section

Measurements

DSC measurements were performed on the Mettler model DSC 822^e. Temperature and enthalpy were calibrated with standard samples of indium (430 K, 3.3 J mol^{-1}) and Zn (692.7 K, 12 J mol^{-1}) by using sealed sample pans. Cooling and heating profiles were recorded and analyzed with a Mettler model STAR^e system. Magnetic susceptibility measurements were performed on a Quantum Design DSM-8 susceptometer equipped with a Quantum Design MPMS-5S SQUID magnetometer at 2000 Oe in the temperature range of 200–360 K. Magnetic data were corrected for magnetization of the sample holder and diamagnetic contributions, which were evaluated from the Pascal constants. Extended EXAFS spectra were recorded in the transmission mode at Beamline 15C of the Photon Factory. A water-cooled Si (311) channel-cut crystal was employed as a monochromator. The intensities of the incident and transmitted X-rays were recorded by using ionization chambers filled with air. The Fe K-edge jump was found to be approximately 1.0, and the total absorption coefficient was estimated to be less than 4.0. Spectra were recorded for a homogeneous pellet sample embedded between two X-ray-transparent polymer films in the range of 7051–7643 eV at every 0.6 eV. The program REX2000 was used for data processing. Rheological measurements were performed on a TA ARES rheometer. Electronic absorption spectra were recorded on a JASCO V-570 spectrometer. Infrared spectra were recorded on a JASCO FTIR-660 plus spectrometer. Variable-temperature infrared spectra were recorded on a JEOL JIR-6000 spectrometer equipped with a JEOL JIR micro 6000 FTIR spectrometer.

Materials

THF was heated at reflux over sodium and benzophenone ketyl under Ar and distilled just before use. The ether 18-crown-6 was recrystallized from acetonitrile, dried overnight under reduced pressure, and then stored under dry N_2. 4-Amino-1,2,4-triazole was recrystallized from THF and stored under N_2. K_2CO_3 was dried at 150 °C under reduced pressure before use. Other reagents were used as received.

Syntheses

1: A mixture of 3,5-bis(dodecan-1-yloxy)benzoic acid, triethylamine (1.3 equiv), and diphenyl (2,3-dihydro-2-thioxo-3-benzoxazolyl)phosphonate (DBOP; 1.3 equiv) in THF was stirred at room temperature for 30 min, and 4-amino-1,2,4-triazole (2.0 equiv) was added to the resulting solution. The reaction mixture was heated at reflux for 30 min, then allowed to cool to room temperature. The resulting suspension was filtered to remove the insoluble 4-amino-1,2,4-triazole, and the filtrate was evaporated to dryness under reduced pressure at room temperature. The residue was purified by chromatography on silica gel ($CHCl_3$/MeOH, 100:0–97:3 *v*/*v*); the second fraction was collected and evaporated to dryness, and the residue was recrystallized from MeOH to give **1** (95 %) as a white powder. FTIR (KBr): $\tilde{\nu}$ = 3115 (ν(NH)), 2920 ($\nu_{asym}(CH_2)$), 2850 ($\nu_{sym}(CH_2)$), 1670 (ν(C=O)), 1605 (ν(C=C)), 1552 (ν(N=C–N)), 1515 (ν-(CONH)), 1468 ($\delta(CH_2)$), 1169 (ν(C–O)), 713 ($\delta(CH_2)$), 631 cm^{-1} (γ-(triazole)); ^{1}H NMR (500 MHz, $CDCl_3$): δ = 0.86 (t, *J* = 7.0 Hz, 6H, CH_3), 1.19–1.30 (m, 32H, $(CH_2)_8$), 1.37–1.43 (m, 4H, $OCH_2CH_2CH_2$), 1.73–1.79 (m, 4H, OCH_2CH_2), 3.92 (t, *J* = 7.0 Hz, 4H, OCH_2), 6.66 (t, *J* = 2.0 Hz, 1H, ArH), 7.17 (d, *J* = 2.0 Hz, 2H, ArH), 8.20 ppm (s, 2H, triazole H); ^{13}C NMR (125 MHz, $CDCl_3$): δ = 14.2, 22.6, 26.1, 29.2, 29.4, 29.5, 29.7, 32.0, 68.5, 106.0, 106.7, 131.8, 143.4, 160.5, 166.0 ppm; MS (MALDI-TOF): *m*/*z* calcd for $C_{33}H_{56}N_4O_3$: 557.8 $[M+H]^+$; found: 557.6.

CHEMISTRY
AN ASIAN JOURNAL

2a: Iron powder and methanesulfonic acid were mixed together in water containing a small amount of ascorbic acid. The reaction mixture was evaporated under reduced pressure to give **2a** as a bluish-white precipitate. FTIR (KBr): $\tilde{\nu}=3400$ (ν(OH)), 1650 (δ(OH)), 1200 (ν_{asym}(O=S=O)), 1100 (ν_{sym}(O=S=O)), 775 (δ_{asym}(O=S=O)), 550 cm^{-1} (δ_{sym}(O=S=O)); elemental analysis: calcd (%) for $C_2H_{12.2}O_{9.1}S_2Fe$: C 7.95, H 4.04; found: C 7.94, H 4.00.

2b: Iron(II) chloride hexahydrate and sodium octanesulfonate were mixed together in water containing a small amount of ascorbic acid. The resulting suspension was filtered, and the white powdery substance isolated was dried over P_2O_5 under reduced pressure to give **2b**. FTIR (KBr): $\tilde{\nu}=3356$ (ν(OH)), 2920 ($\nu_{asym}(CH_2)$), 2847 ($\nu_{sym}(CH_2)$), 1660 (δ(OH)), 1196 (ν_{asym}(S=O)), 1055 cm^{-1} (ν_{sym}(S=O)); elemental analysis: calcd (%) for $C_{16}H_{36}O_8S_2Fe$: C 40.2, H 7.5, S 13.3, Fe 11.6; found: C 39.9, H 7.7, S 13.6, Fe 11.6.

2c: Compound **2c** was obtained by a method similar to that described for **2b**. FTIR (KBr): $\tilde{\nu}=3356$ (ν(OH)), 2920 ($\nu_{asym}(CH_2)$), 2847 ($\nu_{sym}(CH_2)$), 1660 (δ(OH)), 1196 (ν_{asym}(S=O)), 1055 cm^{-1} (ν_{sym}(S=O)); elemental analysis: calcd (%) for $C_{24}H_{54}O_8S_2Fe$: C 50.4, H 9.1, S 10.8, Fe 10.8; found: C 49.1, H 9.3, S 10.8, Fe 10.8.

2d: Compound **2d** was obtained by a method similar to that described for **2b**. FTIR (KBr): $\tilde{\nu}=3356$ (ν(OH)), 2920 ($\nu_{asym}(CH_2)$), 2847 ($\nu_{sym}(CH_2)$), 1660 (δ(OH)), 1196 (ν_{asym}(S=O)), 1055 cm^{-1} (ν_{sym}(S=O)); elemental analysis: calcd (%) for $C_{32}H_{70}O_8S_2Fe$: C 54.7, H 9.9, S 9.1, Fe 7.9; found: C 54.4, H 10.1, S 9.1, Fe 7.9.

3a–d (general procedure): A solution of **2** (5 equiv) in MeOH/THF (5:1) containing a small amount of ascorbic acid was added to a solution of **1** in MeOH/THF (5:1) at 60 °C, and the reaction mixture was stirred for 5 min, then allowed to cool to room temperature. The resulting purple precipitate was collected by filtration, washed with MeOH, and dried under reduced pressure at room temperature to leave **3** as a purple powdery substance in quantitative yield.

3a: FTIR (KBr): $\tilde{\nu}=3446$ (ν(OH)), 3100 (ν(NH)), 2923 ($\nu_{asym}(CH_2)$), 2853 ($\nu_{sym}(CH_2)$), 1696 (ν(C=O)), 1604 (ν(C=C)), 1561 (ν(N=C−N)), 1519 (ν(CONH)), 1465 ($\delta(CH_2)$), 1167 (ν(C−O)), 1206 (ν_{asym}(O=S=O)), 1046 (ν_{sym}(O=S=O)), 776 (δ_{asym}(O=S=O)), 721 ($\delta(CH_2)$), 622 (γ(triazole)), 554 cm^{-1} (δ_{sym}(O=S=O)); elemental analysis: calcd (%) for **3a**·$3H_2O$ ($C_{101}H_{180}N_{12}S_2Fe$): C 61.9, H 8.95, N 8.54, S 3.99, Fe 2.98; found: C 61.1, H 9.07, N 8.05, S 3.0, Fe 2.94.

3b: FTIR (KBr): $\tilde{\nu}=3477$ (ν(OH)), 3095 (ν(NH)), 2924 ($\nu_{asym}(CH_2)$), 2854 ($\nu_{sym}(CH_2)$), 1697 (ν(C=O)), 1602 (ν(C=C)), 1565 (ν(N=C)), 1521 (ν(CONH)), 1466 ($\delta(CH_2)$), 1217 (ν_{asym}(S=O)), 1165 (ν(C−O)), 1105 (δ(triazole C−H)), 1040 (ν_{sym}(S=O)), 860 (γ(triazole)), 603 (γ(triazole)), 545 cm^{-1} (δ_{sym}(S=O)); elemental analysis: calcd (%) for **3b**·$3H_2O$ ($C_{115}H_{210}N_{12}S_2Fe$): C 63.7, H 9.32, N 7.75, S 2.95, Fe 2.57; found: C 63.7, H 9.93, N 7.8, S 3.0, Fe 2.55.

3c: FTIR (KBr): $\tilde{\nu}=3477$ (ν(OH)), 3093 (ν(NH)), 2923 ($\nu_{asym}(CH_2)$), 2853 ($\nu_{sym}(CH_2)$), 1697 (ν(C=O)), 1602 (ν(C=C)), 1561 (ν(N=C)), 1523 (ν(CONH)), 1466 ($\delta(CH_2)$), 1217 (ν_{asym}(S=O)), 1165 (ν(C−O)), 1105 (δ(triazole C−H)), 1039 (ν_{sym}(S=O)), 860 (γ(triazole)), 603 (γ(triazole)), 526 cm^{-1} (δ_{sym}(S=O)); elemental analysis: calcd (%) for **3c**·$6.6H_2O$ ($C_{123}H_{231.2}N_{12}S_2Fe$): C 64.5, H 10.1, N 7.34, S 2.79, Fe 2.43; found: C 65.5, H 10.1, N 7.2, S 2.9, Fe 2.38.

3d: FTIR (KBr): $\tilde{\nu}=3445$ (ν(OH)), 3093 (ν(NH)), 2922 ($\nu_{asym}(CH_2)$), 2853 ($\nu_{sym}(CH_2)$), 1695 (ν(C=O)), 1603 (ν(C=C)), 1563 (ν(N=C)), 1524 (ν(CONH)), 1466 ($\delta(CH_2)$), 1213 (ν_{asym}(S=O)), 1166 (ν(C−O)), 1105 (δ(triazole C−H)), 1039 (ν_{sym}(S=O)), 860 (γ(triazole)), 603 (γ(triazole)), 526 cm^{-1} (δ_{sym}(S=O)); elemental analysis: calcd (%) for **3d**·$7.5H_2O$ ($C_{131}H_{249}N_{12}S_2Fe$): C 65.05, H 9.65, N 6.95, S 2.6, Fe 2.3; found: C 65.05, H 10.2, N 6.6, S 2.9, Fe 2.6.

Acknowledgements

We thank Dr. K. Okitsu of the High Power X-Ray Laboratory (University of Tokyo) for EXAFS measurements under the approval of the Photon Factory Program Advisory Committee (No. 2003G203). T.F. thanks the JSPS Research Fellowships for Young Scientists.

[1] a) E. König. G. Ritter, S. K. Kulshreshtha, *Chem. Rev.* **1985**, *85*, 219–234; b) J. A. Real, A. B. Gaspar, V. Niel, M. C. Muñoz, *Coord. Chem. Rev.* **2003**, *236*, 121–141; c) R. Boca, W. Linert, *Monatsh. Chem.* **2003**, *134*, 199–216; d) P. J. von Koningsbruggen, M. Grunert, P. Weinberger, *Monatsh. Chem.* **2003**, *134*, 183–198.

[2] a) O. Kahn, J. Kröber, C. Jay, *Adv. Mater.* **1992**, *4*, 718–728; b) O. Kahn, J. P. Launay, *Chemtronics* **1988**, *3*, 140–151; c) O. Kahn, C. Jay, *Science* **1998**, *279*, 44–48; d) P. Gütlich, H. A. Goodwin, *Top. Curr. Chem.* **2004**, *233–235*.

[3] a) N. Sasaki, T. Kambara, *J. Chem. Phys.* **1981**, *74*, 3472–3481; b) H. Spiering, E. Meissner, H. Köppen, E. W. Müller, P. Gütlich, *Chem. Phys.* **1982**, *68*, 65–71.

[4] a) G. Schwarzenbacher, M. S. Gangl, M. Goriup, M. Winter, M. Grunert, F. Renz, W. Linert, R. Saf, *Monatsh. Chem.* **2001**, *132*, 519–529; b) O. Roubeau, B. Agricole, R. Clerac, S. Ravaine, *J. Phys. Chem. B* **2004**, *108*, 15110–15116; c) O. Roubeau, A. Colin, V. Schmitt, R. Clerac, *Angew. Chem.* **2004**, *116*, 3345–3348; *Angew. Chem. Int. Ed.* **2004**, *43*, 3283–3286; d) Y. Galyametdinov, V. Ksenofontov, A. Prosvirin, I. Ovchinnikov, G. Ivanova, P. Gütlich, W. Haase, *Angew. Chem.* **2001**, *113*, 4399–4401; *Angew. Chem. Int. Ed.* **2001**, *40*, 4269–4271; e) Y. Bodenthin, U. Pietsch, H. Möhwald, D. G. Kurth, *J. Am. Chem. Soc.* **2005**, *127*, 3110–3115; f) M. Seredyuk, A. B. Gaspar, V. Ksenofontov, S. Reiman, Y. Galyametdinov, W. Haase, E. Rentschler, P. Gütlich, *Chem. Mater.* **2006**, *18*, 2513–2519.

[5] a) T. Fujigaya, D. L. Jiang, T. Aida, *J. Am. Chem. Soc.* **2005**, *127*, 5484–5489; b) T. Fujigaya, D.-L. Jiang, T. Aida in *Novel Strategies for Fundamental Innovation in Polymer Science* (Ed.: N. Naga), Research Signpost, Kerala, **2005**, pp. 165–176.

[6] V. P. Sinditskii, V. I. Sokol, A. E. Fogel'zang, M. D. Dutov, V. V. Serushkin, M. A. Porai-Koshits, B. S. Svtelov, *Russ. J. Inorg. Chem.* **1987**, *32*, 1149–1152.

[7] The jump in the magnetic moment of the gel upon heating corresponds to 85% of that of the solid sample of **3c**, in which 96% of the iron(II) species undergoes spin crossover.

[8] a) P. J. von Koningsbruggen, Y. Garcia, E. Codjovi, R. Lapouyade, O. Kahn, L. Fournes, L. Rabardel, *J. Mater. Chem.* **1997**, *7*, 2069–2075; b) Y. Garcia, P. J. von Koningsbruggen, E. Codjovi, R. Lapouyade, O. Kahn, L. Rabardel, *J. Mater. Chem.* **1997**, *7*, 857–858; c) O. Roubeau, J. G. Haasnoot, E. Codjovi, F. Varret, J. Reedijk, *Chem. Mater.* **2002**, *14*, 2559–2566.

[9] D. Bougeard, N. Calvé, B. Roch, A. Novak, *J. Chem. Phys.* **1976**, *64*, 5152–5164.

[10] For CH–O interactions, see: a) R. Taylor, O. Kennard, *J. Am. Chem. Soc.* **1982**, *104*, 5063–5070; b) P. Dauber, A. T. Hagler, *Acc. Chem. Res.* **1980**, *13*, 105–112; c) G. R. Desiraju, *Acc. Chem. Res.* **1991**, *24*, 290–296; for SO_3^-–H_2O interactions, see: E. Coronado, J. R. Galán-Mascarós, A. Murcia-Martínez, F. M. Romero, A. Tarazón in *NATO ASI Series* (Eds.: L. Ouahab and E. Yagubskii), Kluwer Academic Publishers, Norwell, **2004**, Vol. 139, p. 127; d) M. Laporta, M. Pegraron, L. Zanderighi, *Phys. Chem. Chem. Phys.* **1999**, *1*, 4619–4624.

Received: November 8, 2006
Published online: December 14, 2006

